

Tetraaryl-methane analogues in group 14—V. Distortion of tetrahedral geometry in terms of through-space π – π and π – σ interactions and NMR sagging in terms of π – σ^* charge transfer

Michael Charissé^a, Andrea Zickgraf^a, Heike Stenger^a, Elmar Bräu^a,
Cristelle Desmarquet^a, Martin Dräger^{a,*}, Silke Gerstmann^b,
Dainis Dakternieks^{b,*} and James Hook^c

^aInstitut für Anorganische Chemie und Analytische Chemie der Johannes Gutenberg-Universität,
D-55099 Mainz, Germany

^bSchool of Biological and Chemical Sciences, Faculty of Science and Technology, Deakin University,
Geelong, Vic. 3217, Australia

^cNMR Facility, The University of New South Wales, Sydney, NSW 2052, Australia

(Received 24 February 1998; accepted 23 June 1998)

Abstract—44 members of the compound series $\text{Ph}_{4-n}\text{MR}_n$ ($M = \text{Si, Ge, Sn, Pb}$; $R = o-, m-, p\text{-Tol}$; $n = 0-4$) were synthesized (15 new compounds). The crystal structures of $\text{Ph}_3\text{Sn}(o\text{-Tol})$ and $\text{PhSn}(o\text{-Tol})_3$ were determined and compared to 16 known structures. Subject to the distance $d(\text{M}-\text{C})$, an interplay between through-space π – π repulsion and π – σ attraction leads to either elongated or compressed tetrahedral geometry. ^{29}Si -, ^{119}Sn - and ^{207}Pb -NMR chemical shifts were determined in solution and in the solid state. ^{73}Ge chemical shifts were measured only in solution. An upfield or downfield sagging of the chemical shifts along each series is rationalized in terms of a π – σ^* charge transfer which is constrained by torsion of the aromatic groups. © 1998 Elsevier Science Ltd. All rights reserved

Keywords: silicon; germanium; tin; lead; through-space interaction; heteronuclear NMR in solution and solid state; π – σ^* charge transfer.

INTRODUCTION

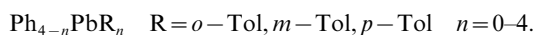
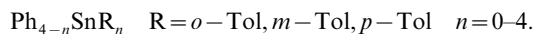
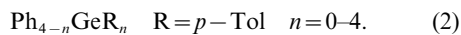
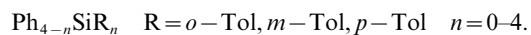
As part of ongoing studies about tetraarylmethane analogues [1–4], the series of compounds $\text{Ph}_{4-n}\text{M}(p\text{-Tol})_n$ ($M = \text{Si, Ge, Sn, Pb}$; $n = 0-4$) was synthesized and investigated using X-ray diffraction and NMR spectroscopy [1]. The structural finding of elongated tetrahedra for $M = \text{Si}$ and Ge and compressed tetrahedra for $M = \text{Sn}$ and Pb (see Ref. [5]) was rationalized by means of an interplay between π – σ attractions and π – π repulsions of the aromatic groups [1, 6, 7]. The sagging effect (see Refs. [8–10]) observed in

the solution state ^{29}Si -, ^{119}Sn - and ^{207}Pb -NMR chemical shifts was rationalized by means of a π – σ^* charge transfer from the aromatic groups into the LUMO associated mostly with the hetero atom M [1].

In this paper the subject is extended synthetically to the groups *o*- and *m*-tolyl [four series of compounds $\text{Ph}_{4-n}\text{MR}_n$, (1–4)]. In addition to the 16 crystal structures known previously [1–4], the structures of $\text{Ph}_3\text{Sn}(o\text{-Tol})$ and $\text{PhSn}(o\text{-Tol})_3$ were determined. Heteronuclear NMR chemical shifts in solution and also in the solid state were determined for all compounds of series eq. (1), eq. (3) and eq. (4). In addition, ^{73}Ge -NMR chemical shifts for the five compounds of series eq. (2) in solution are given [11–16]. Semi-empirical MO calculations have been done to support the concept of a π – σ^* charge transfer. As will be seen from

* Author to whom correspondence should be addressed.
Tel.: +49-6131-395757; Fax: +49-6131-395380.

the results, these exhaustive calculations concluded to be altogether unrewarding and fruitless.



RESULTS AND DISCUSSION

Structural results

Figure 1 shows the molecular structures of $\text{Ph}_3\text{Sn}(o\text{-Tol})$ and of $\text{PhSn}(o\text{-Tol})_3$. Relevant bond lengths and

angles are listed in Table 1. Both molecules possess crystallographically a S_4 symmetry, i.e. the ortho methyl groups exhibit a statistical disorder. One of the four possible ordered arrangements is given in Fig. 1, respectively.

As outlined for tetraaryls with phenyl and *p*-tolyl substitution [1], the tetrahedra with $\text{M} = \text{C}, \text{Si}, \text{Ge}$ are elongated (two bond angles less and four bond angles greater than 109.5°) whereas the tetrahedra with $\text{M} = \text{Sn}, \text{Pb}$ are compressed (two bond angles greater and four bond angles less than 109.5°). This result is valid also for the cases of *o*-tolyl and *m*-tolyl substitution. Figure 2 gives a plot of $d(\text{M}-\text{C})$ vs the twofold angle $\Phi(\text{C}-\text{M}-\text{C})-[2x]$ for all 18 cases $\text{Ph}_{4-n}\text{MR}_n$, which have been investigated by X-ray crystallography. At $d(\text{M}-\text{C}) = 2.06 \text{ \AA}$ (cubic fit curve) an overall repulsion between the aromatic groups transforms into an overall attraction. For short $\text{M}-\text{C}$ distances the through-space $\pi-\pi$ repulsion predominates; for long $\text{M}-\text{C}$ distances the through-space $\pi-\sigma$ attraction prevails.

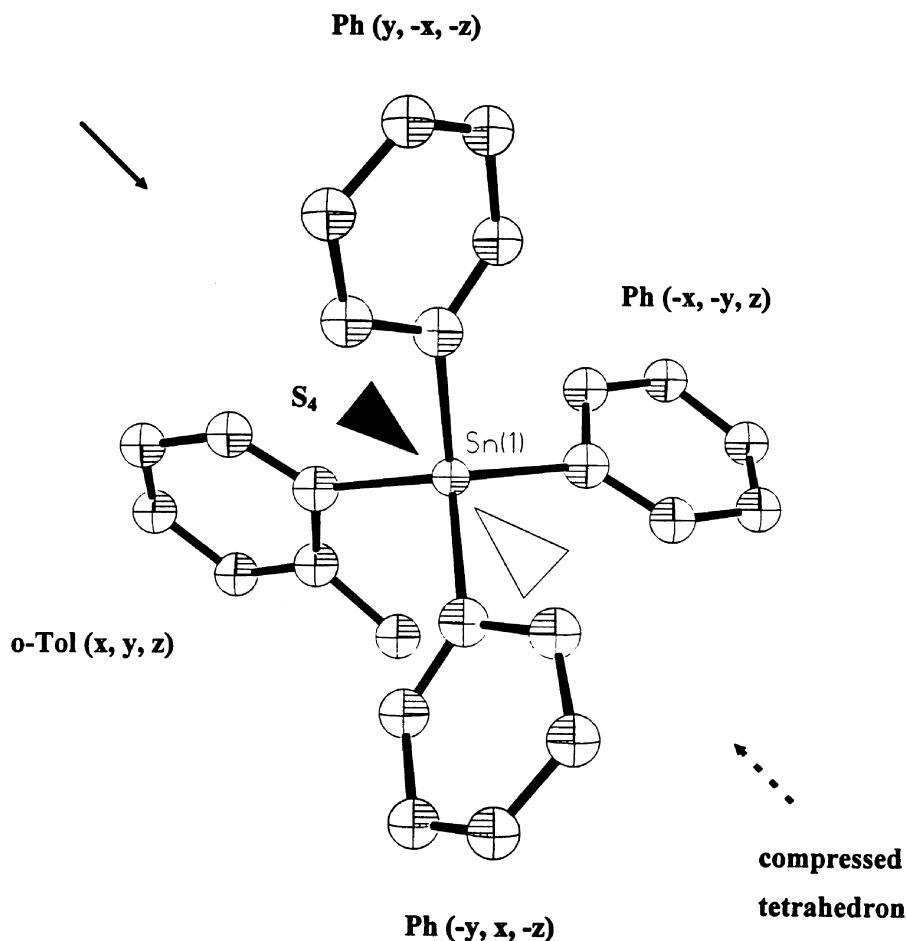
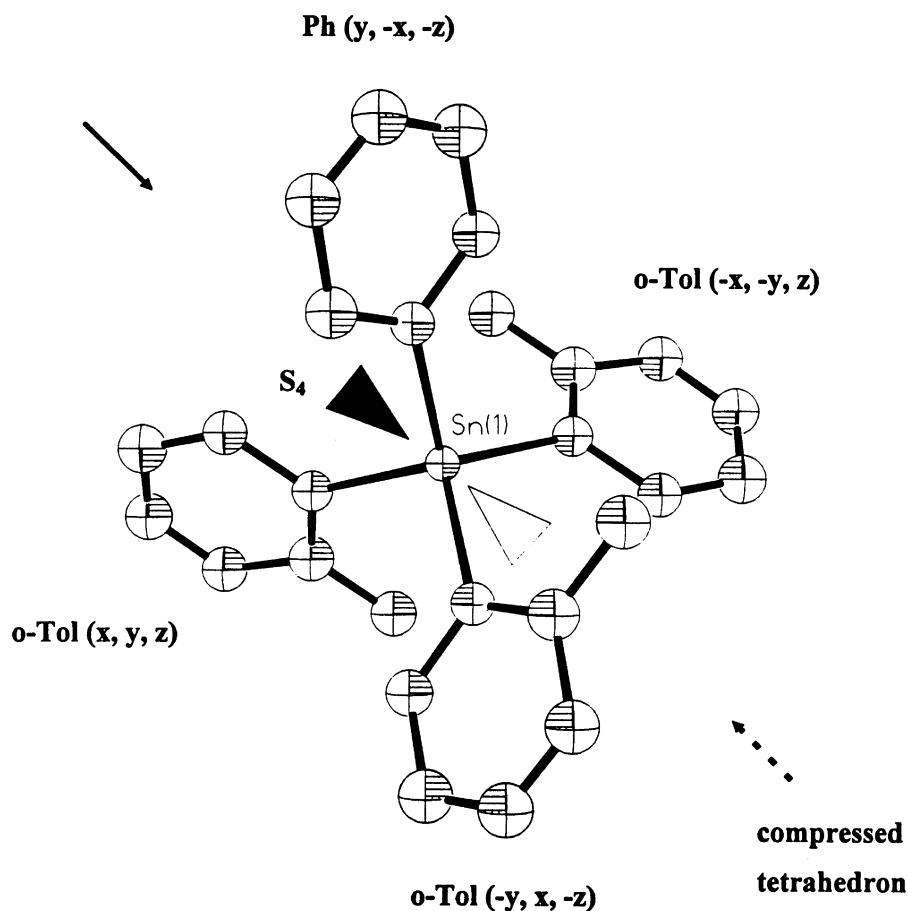


Fig. 1. Ortep drawings of $\text{Ph}_3\text{Sn}(o\text{-Tol})$ (top) and of $\text{PhSn}(o\text{-Tol})_3$ (continued). Only one of the four possible ordered arrangements is given, respectively. Thermal ellipsoids are at the 20% probability level; hydrogen atoms are omitted for better clarity. The molecules are compressed along the outlined pseudo S_4 axes. The group identifications include the symmetry operators of the space group $P4_21c$.

Fig. 1. *Continued.*Table 1. Bond lengths (Å) and bond angles (°) of $\text{Ph}_3\text{Sn}(o\text{-Tol})$ and $\text{PhSn}(o\text{-Tol})_3$ and of Ph_4Sn and $\text{Sn}(o\text{-Tol})_4$ ^a for comparison (all compounds crystallize in the space group $P4_2/c$)

Compound	Distance Sn–C(1)	Two-fold angle C(1)–Sn–C(1a) $\Phi(\text{C–Sn–C})_{2\times}$	Four-fold angle C(1)–Sn–C(1b) $\Phi(\text{C–Sn–C})_{4\times}$
Ph_4Sn	2.139(4)	111.2(2)	108.6(1)
$\text{Ph}_3\text{Sn}(o\text{-Tol})$	2.09(4)	111(2)	109(1)
$\text{PhSn}(o\text{-Tol})_3$	2.157(8)	112.8(4)	107.8(4)
$\text{Sn}(o\text{-Tol})_4$	2.152(5)	112.6(3)	107.9(1)

^a See Ref. [17].

NMR chemical shifts

Table 2 gives the heteronuclear NMR chemical shifts for the homoleptic and heteroleptic tetraaryls $\text{Ph}_{4-n}\text{MR}_n$ in CDCl_3 solution. The series eq. (2) is the first systematic investigation of ^{73}Ge -NMR chemical shifts, which has been described (Figure 3) [11–16].

Table 3 gives the solid state ^{29}Si , ^{119}Sn and ^{207}Pb chemical shifts of the compounds of the series eqs. (1, 3–4). Figure 4 shows exemplarily for $\text{M}=\text{Sn}$ the six sequences of $\delta(^{119}\text{Sn})$ in the solution (top) and in the solid (bottom) state. The values are connected by cubic fit curves.

With regard to the aliphatic compounds Me_4M ,

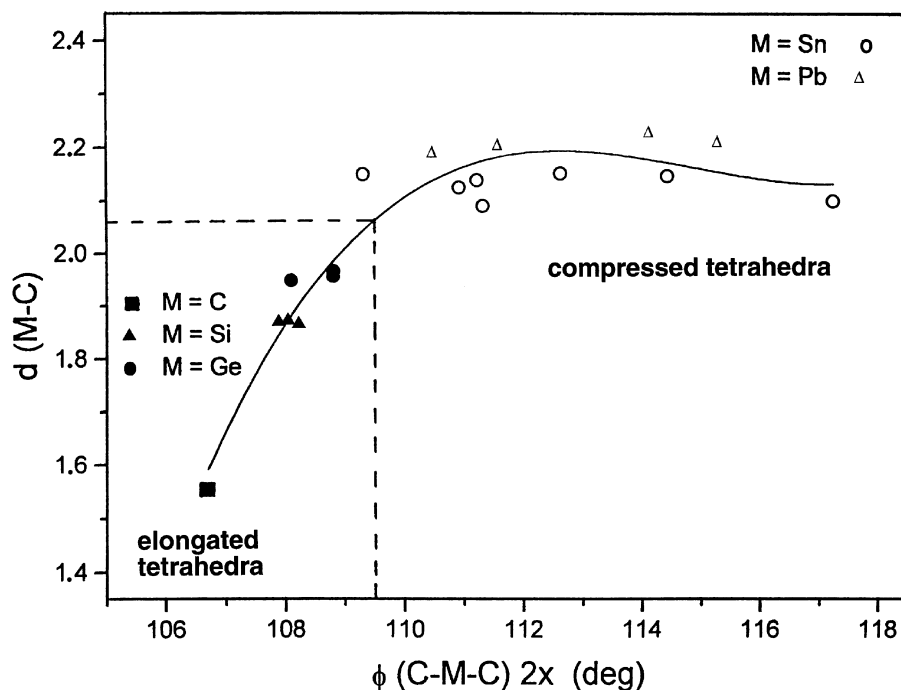


Fig. 2. Plot of the bond distances $d(\text{M}-\text{C})$ (Å) vs the two-fold bond angle $\Phi(\text{C}-\text{M}-\text{C})-2 \times$ (°) for 18 compounds $\text{Ph}_{4-n}\text{MR}_n$ ($\text{M} = \text{C}, \text{Si}, \text{Ge}, \text{Sn}, \text{Pb}$; $\text{R} = o-, m-, p\text{-Tol}$; $n = 0-4$) in relation to the distortion of the tetrahedra around M. Data from Ref. [1-4] and references cited therein. Cubic fit curve (change of distortion at 2.06 Å).

Table 2. Solution-state ^{29}Si -, ^{73}Ge -, ^{119}Sn - and ^{207}Pb - NMR chemical shifts (ppm^a) for the series $\text{Ph}_{4-n}\text{MR}_n$ eqs. (1-4)

M	R	Ph_4M	Ph_3MR	Ph_2MR_2	PhMR_3	MR_4
Si	<i>o</i> -Tol	-13.98	-14.39	-13.90	-13.42	-12.52
	<i>m</i> -Tol		-14.25	-14.24	-14.23	-14.34
	<i>p</i> -Tol		-14.29	-14.36	-14.42	-14.55
Ge	<i>p</i> -Tol	-32.90	-32.49	-31.71	-30.77	-31.24
Sn	<i>o</i> -Tol	-128.1	-126.7	-124.7	-121.7	-124.5
	<i>m</i> -Tol		-130.2	-130.1	-130.0	-129.8
	<i>p</i> -Tol		-129.1	-127.7	-126.1	-124.6
Pb	<i>o</i> -Tol	-179.0	-170.4	-161.2	-152.9	-166.7
	<i>m</i> -Tol		-181.5	-180.9	-180.3	-179.5
	<i>p</i> -Tol		-179.5	-176.3	-174.0	-171.3

^a Solvent CDCl_3 ; relative to the external standards $\text{Me}_4\text{Si}/\text{Ge}/\text{Sn}/\text{Pb}$, respectively, ambient temperature.

the chemical shifts $\delta(^{29}\text{Si}/^{73}\text{Ge}/^{119}\text{Sn}/^{207}\text{Pb})$ of the homoleptic members Ph_4M and MTol_4 are all upfield and this shielding had been explained by a $\pi(\text{aromatic}) \rightarrow \sigma^*(\text{M})$ charge transfer¹ [1]. Between the

¹ A seeming exception is Ph_4C with $\delta(^{13}\text{C}) = +65.0$ ppm ($\text{Me}_4\text{C} + 28.0$ ppm). The central carbon atom has four short distances (cf. Figure 2) to the deshielding side-on position of the aromatic ring current [1].

homoleptic end members Ph_4Sn and SnR_4 , a sagging pattern [8-10] holds. The sagging effect is different for the solution and for the solid state. Furthermore, the effect changes from the (*o*-Tol) to the (*m*-Tol) to the (*p*-Tol) series. A possible explanation may be that $\pi-\sigma^*$ charge transfer depends on the torsion of the aromatic groups about the $\text{M}-\text{C}_{\text{ipso}}$ axis. In solution the torsion angles easily arrange themselves, such as, to optimize the energetic interactions among

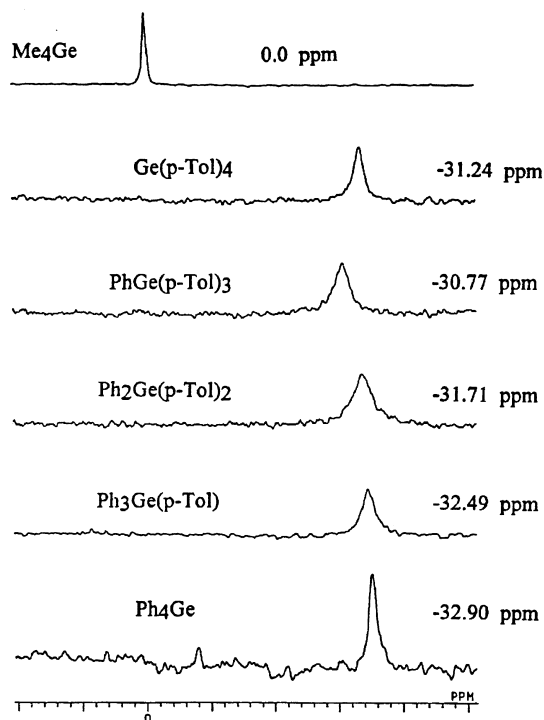


Fig. 3. ^{73}Ge -NMR spectra for the series of compounds $\text{Ph}_{4-n}\text{Ge}(p\text{-Tol})_n$ in CDCl_3 solution. Chemical shifts are given with reference to Me_4Ge .

the four aromatic groups whereas in the solid state the torsion angles are constrained by the crystal packing [7]. In solution, the sterically undemanding groups *m*-tolyl and *p*-tolyl lead to an upfield sagging (excess of charge, with regard to a linear course). On the other hand, the sterically crowded *o*-tolyl group leads to a distinct downfield sagging (shortage of charge).

In accordance with the similar molecular forms of the compounds with $\text{M} = \text{Sn}$ and Pb (see Section structural results), the three solution state $\delta(^{207}\text{Pb})$ sagging curves are nearly identical to those of $\delta(^{119}\text{Sn})$ (Table 2 and Fig. 4). Also the three solid state $\delta(^{207}\text{Pb})$ sagging curves show a close correspondence to those of $\delta(^{119}\text{Sn})$. Similar torsions of the aromatic groups and similar crystal structures can be assumed.

In solution the $\delta(^{73}\text{Ge})$ and $\delta(^{29}\text{Si})$ sagging curves show similar trends to those described for $\delta(^{119}\text{Sn})$ and $\delta(^{207}\text{Pb})$. The shortage of charge (downfield shift) is enhanced for the case of the sterically very demanding *o*-tolyl group at Si. However the known solid state structures of the Si series are different and this fact manifests itself in sagging curves definitely different from those of Fig. 4.

Semi-empirical MO calculations

To support the concept of a $\pi\text{-}\sigma^*$ charge transfer, semi-empirical MO calculations at the PM3 level (MOPAC 6.0 program package, parameter set: [18, 19] (all 44 compounds $\text{Ph}_{4-n}\text{MR}_n$, molecular geometries optimized starting from the known crystal structures) and at the Extended Hückel level [20] ($\text{PhSn}(o\text{-Tol})_3$, fixed geometry of the structure determination) were performed. The results are similar for all compounds. On the basis of the main coefficients, the energetic sequences of the MO's are in the order eq. (5). With regard to this order, a definite higher transition probability is needed for the assumed $\pi\text{-}\sigma^*$ charge transfer (high energy gap) than for a $\pi\text{-}\pi^*$ charge transfer (low energy gap) [21] (A quantitative correspondence between the PM3 energy differences and the energies of the experimental UV bands between 240 and 270 nm does not exist.)

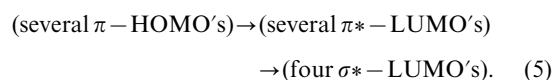


Table 3. Solid-state ^{29}Si -, ^{119}Sn -, and ^{207}Pb -NMR chemical shifts (ppm^a) for the series $\text{Ph}_{4-n}\text{MR}_n$ eqs. (1, 3–4)

M	R	Ph_4M	Ph_3MR	Ph_2MR_2	PhMR_3	MR_4
Si	<i>o</i> -Tol	-14.07	-14.08	-17.01 ^b	-14.79	-13.37
	<i>m</i> -Tol		-12.81	-13.26	-12.65	-12.03
	<i>p</i> -Tol		-14.60	-13.75	-13.48	-13.31
Sn	<i>o</i> -Tol	-121.1	-123.1	-122.1	-123.6	-127.4
	<i>m</i> -Tol		-120.2	-115.2	-111.4	-107.5
	<i>p</i> -Tol		-119.9	-117.7	-118.8	-118.8
Pb	<i>o</i> -Tol	-146.7	-146.9	-151.1	-150.2	-159.5
	<i>m</i> -Tol		-147.8	-146.4	-128.0	-119.3
	<i>p</i> -Tol		-145.9	-142.0	-150.0	-148.8

^a Conditions as given in Section 3.

^b Additional trace signal at -14.7 ppm.

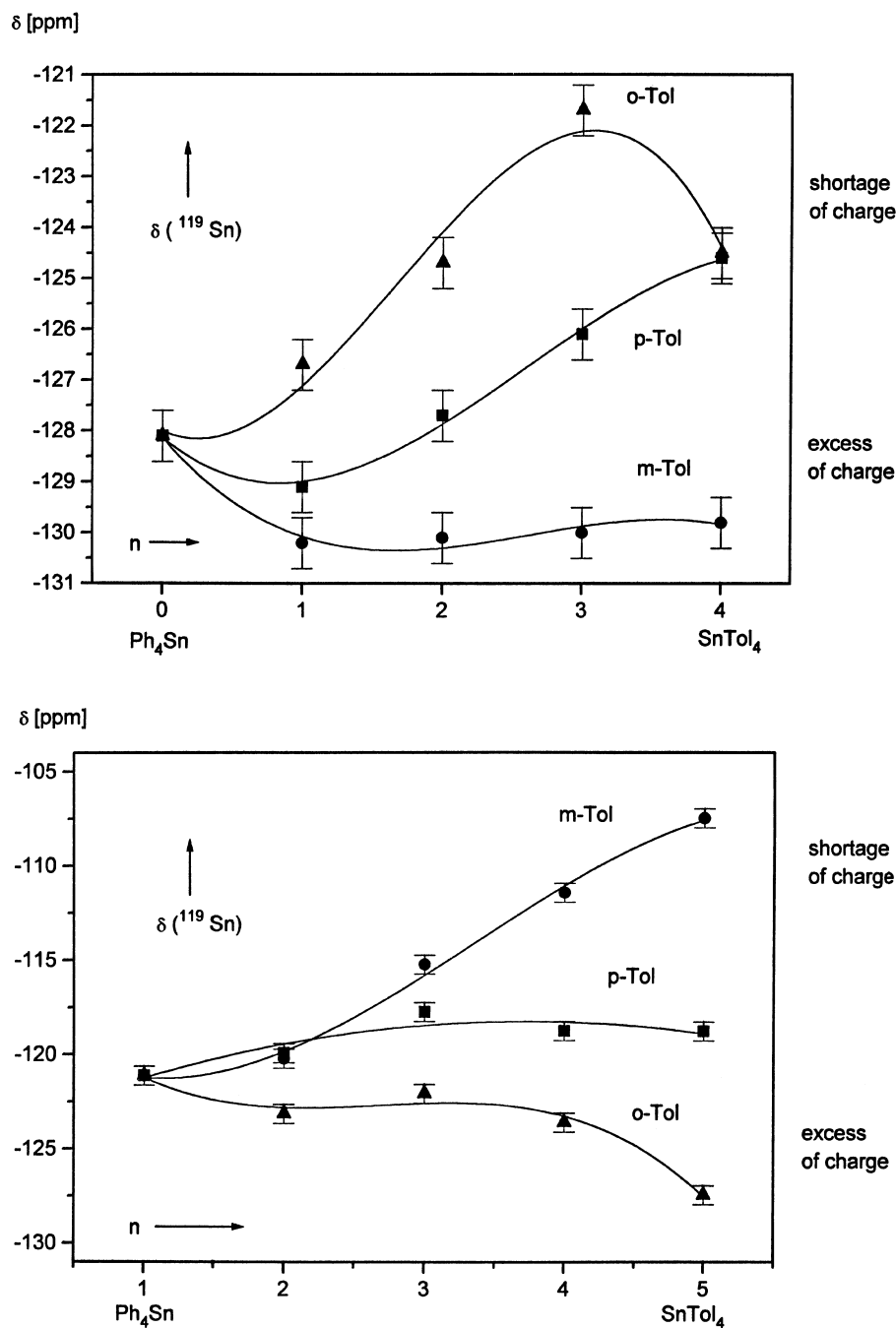


Fig. 4. Course of ^{119}Sn -NMR chemical shifts vs n for the series of compounds $\text{Ph}_{4-n}\text{SnR}_n$ ($\text{R} = o-, m-, p\text{-Tol}$; $n = 0-4$) in CDCl_3 solution (top) and in the solid state (bottom). Cubic fit curves.

In detail, all PM3 calculations result in the energetic σ^* -LUMO sequences eq. (6). With regard to the NMR behavior of eqs. (1-4), no definite order or correlation exist with $E(\sigma^*\text{-LUMO})$ or with its difference to the π -HOMO, apart from the fact that the MO sequences are most disturbed if the group (*o*-Tol) is involved.

$$E(\text{Si}) > E(\text{Pb}) > E(\text{Sn}) > E(\text{Ge}). \quad (6)$$

In fact, it can be concluded that semi-empirical calculations have to lower a sophistication, to be of any purpose in discussing the postulated π - σ^* charge transfer.

EXPERIMENTAL

Synthesis

The 14 homoleptic compounds and the 12 heteroleptic *p*-tolyl compounds were prepared by literature methods [1–4]. For previous work on the *o*-tolyl substituted silicon compounds, see Ref. [22–25]. The mixed ortho- and meta-substituted tin and lead compounds $\text{Ph}_{4-n}\text{M}(\text{o-}, \text{m-Tol})_n$ ($n=1-3$; $\text{M}=\text{Sn}, \text{Pb}$) were synthesized via a Grignard reaction with the corresponding halides $\text{Ph}_{4-n}\text{MX}_n$ ($\text{X}=\text{Cl}, \text{Br}, \text{I}$). Compounds of the series $\text{Ph}_{4-n}\text{SiM}(\text{m-Tol})_n$ ($n=1-3$) were obtained by reaction of $\text{Ph}_{4-n}\text{SiCl}_n$ with $\text{Li}(\text{m-Tol})$. A representative detailed procedure follows for the compound $\text{PhGe}(\text{p-Tol})_3$, which had been described in Ref. [1] as contaminated with $\text{Ge}_2(\text{p-Tol})_6$. To 15.6 mmol of $(\text{p-Tol})\text{Li}$ in 50 ml ether is slowly added, at ambient temperature 1.02 g (4 mmol) of freshly distilled PhGeCl_3 , dissolved in 50 ml ether. After 1 h under reflux, the ether is distilled off and substituted continuously by toluene. After further stirring for 4 h under reflux and for 20 h at ambient temperature, the solution is hydrolyzed by slow addition of 1 M HCl. The organic layer is dried with Na_2SO_4 , the solvent distilled off and methanol added. The crude product is separated by filtration, washed with cold methanol and recrystallized from methanol/toluene (3:1). Table 4 summarizes the results obtained in this study.

Melting points were determined in glass capillaries in a Kofler melting block. Elemental analyses (C and H) were obtained from the Institut für Organische Chemie, Universität Mainz, with a Perkin-Elmer CHN-Analyser 240.

Crystal structure determinations

Colorless single crystals of $\text{Ph}_3\text{Sn}(\text{o-Tol})$ and $\text{PhSn}(\text{o-Tol})_3$ were obtained by slow evaporation of a CDCl_3 solution. As previously [1–4], the crystals of the heteroleptic compounds were all of a poor quality. An inspection by means of Weissenberg exposures was essential. Both eventually chosen crystals had a low diffraction power. A summary of crystal data, intensity data collections and refinements, is given in Table 5. The crystals were fixed with glue and sealed in thin-walled glass capillaries. The experimental densities were determined by flotation in an aqueous polytungstate solution. Integrated intensities were collected on an Enraf-Nonius CAD4 diffractometer.

Both compounds crystallize in the same tetragonal space group $\text{P}\bar{4}2_1\text{c}$ as their homoleptic end members (see the first footnote of Table 5). Trials of refinement in a monoclinic setting resulted in distinctly worse geometries and esd's. The space group symmetry requires a S_4 symmetry for both molecules, i.e. the ortho-methyl groups are statistically disordered (site occupations 0.25 and 0.75, respectively). On account

of the small number of reflections of significant intensity, only the Sn atom was given anisotropic thermal parameters, the C atoms were handled isotropically. The hydrogen atoms were calculated as riding on their carbon atoms. For calculations and drawings local versions of SHELX-76 and ORTEP were used. Tables listing details of crystal data and structure determinations, full sets of parameters (Sn, C and H), all bond lengths and angles and torsion angles and labelled plots have been deposited at the Cambridge Crystallographic Data Centre as supplementary material.

Solution state NMR

^{29}Si -, ^{119}Sn - and ^{207}Pb -NMR spectra were recorded on a Bruker WP 80/DS instrument (digital resolution 0.5 Hz) at 15.92 MHz (^{29}Si), 29.88 MHz (^{119}Sn) and 16.74 MHz (^{207}Pb). Solution state ^{73}Ge -NMR spectra were recorded on a Jeol JNM-GX 270 spectrometer (frequency 9.3 MHz, sweep width 2000 Hz, acquisition time 2 s, scans 1500). The chemical shifts are relative to the external standards Me_4Si , Me_4Ge , Me_4Sn and Me_4Pb . Solutions of 100–400 mg of compound/3 mL of CDCl_3 were used.

Solid state NMR

^{29}Si -, ^{119}Sn - and ^{207}Pb -NMR spectra were measured on a Bruker MSL-300S spectrometer operating at 59.641, 111.922 and 62.55 MHz, respectively. Samples of 300 mg of the organosilicon and lead compounds were packed into 7 mm zirconia rotors and spun at the magic-angle, at speeds of 2.5 kHz. The organotin compounds (*ca.* 100 mg) were measured in 4 mm zirconia rotors at 5 kHz. Spectra were obtained with broad-band double air-bearing cross-polarization Bruker WB-BL probes, at ambient temperature (295 K) from single contact cross-polarization (CP) experiments.

Solid state ^{29}Si -NMR: spectral width, 20 kHz; pulse width, 5.5 μs (90°) ^1H pulse; contact time, 1 ms; recycle time, 20 s; chemical shifts with respect to kaolinite ($\delta(^{29}\text{Si}) = -91.5$ ppm (Q^3 connected Si) [26, 27]; set up of the CP conditions and use as an external standard. Solid state ^{119}Sn -NMR: spectral width, 33 kHz; pulse width, 4.0 μs (90°) ^1H pulse; contact time, 10 ms; recycle time, 10 s; chemical shifts with respect to $\text{Sn}(\text{c-Hex})_4$ ($\delta(^{119}\text{Sn}) = -97.4$ ppm [28]; set up of the CP conditions and use as an external standard. Acquisition of 128 scans was sufficient to obtain spectra with a satisfactory signal to noise ratio. Solid state ^{207}Pb -NMR: spectral width, 62.5 kHz; pulse width, 3.5–4.0 μs (90°) ^1H pulse; contact time, 5–20 ms; recycle time, 30 s; chemical shifts with respect to $\text{Pb}(\text{p-Tol})_4$ ($\delta(^{207}\text{Pb}) = -148.8$ ppm [29, 30]; set up of the CP conditions and use as an external standard). Acquisition of 64–128 scans was sufficient to obtain spectra with a satisfactory signal to noise ratio.

Table 4. Experimental data and analytical results for the series Ph_{4-n}MR_n

Products	Preparation ^a initial compounds solvent; T [time (h)]	Recryst. from	Yield (%)	M.P. (°C) (lit.)	Formula M _r	Elemental analysis (%) C _{obs} (C _{calc}) H _{obs} (H _{calc})
Ph ₃ Si(<i>o</i> -Tol)	Ph ₃ SiCl ₂ / <i>o</i> -Tol)Li ether; RT (15)	EtOH/toluene	38	175–180 (186–187 ^b)	C ₂₅ H ₂₂ Si 350.54	85.43 (85.66) 6.28 (6.33)
Ph ₂ Si(<i>o</i> -Tol) ₂	Ph ₂ SiCl ₂ / <i>o</i> -Tol)Li ether; RT (15) + refl. (2)	toluene/PE(1:5) ^c	14	172 (174 ^b)	C ₂₆ H ₂₄ Si 364.56	85.10 (85.66) 6.61 (6.64)
PhSi(<i>o</i> -Tol) ₃	(<i>o</i> -Tol) ₃ SiCl/PhLi ether; refl. (50)	EtOH/toluene	48	186–190 (195 ^b)	C ₂₇ H ₂₆ Si 378.59	85.45 (85.66) 6.85 (6.92)
Si(<i>o</i> -Tol) ₄	(<i>o</i> -Tol) ₃ SiCl/ <i>o</i> -Tol)Li ether; refl. (48) + neat (6 ^d)	toluene/PE(1:4) ^e	10	218–224 ^c (228 ^c)	C ₂₈ H ₂₈ Si 392.62	85.45 (85.66) 7.21 (7.19)
Ph ₃ Si(<i>m</i> -Tol)	Ph ₃ SiCl/ <i>m</i> -Tol)Li ether; RT (15) + refl. (1)	EtOH/toluene	51	143	C ₂₅ H ₂₂ Si 350.54	85.25 (85.66) 6.38 (6.33)
Ph ₂ Si(<i>m</i> -Tol) ₂	Ph ₂ SiCl ₂ / <i>m</i> -Tol)Li ether; RT (15) + refl. (1)	EtOH/toluene	37	116	C ₂₆ H ₂₄ Si 364.56	84.97 (85.66) 6.09 (6.64)
PhSi(<i>m</i> -Tol) ₃	PhSiCl ₂ / <i>m</i> -Tol)Li ether; RT (15) + refl. (1)	EtOH/toluene	55	126	C ₂₇ H ₂₆ Si 378.59	85.74 (85.66) 6.93 (6.92)
PhGe(<i>p</i> -Tol) ₃	PhGeCl ₃ / <i>p</i> -Tol)Li ether; RT (20) + refl. (4)	MeOH/toluene	65	181–182 (106–107 ^f)	C ₂₇ H ₂₆ Ge 423.09	76.53 (76.56) 6.40 (6.19)
Ph ₃ Sn(<i>o</i> -Tol)	Ph ₃ SnCl/ <i>o</i> -Tol)MgBr THF; RT (1) + refl. (17)	EtOH/toluene	85	162–163	C ₂₅ H ₂₂ Sn 441.14	67.88 (68.07) 5.11 (5.03)
Ph ₂ Sn(<i>o</i> -Tol) ₂	Ph ₂ SnCl ₂ / <i>o</i> -Tol)MgBr THF; RT (1) + refl. (15)	EtOH/toluene	50	148–149	C ₂₆ H ₂₄ Sn 455.17	68.57 (68.61) 5.41 (5.31)
PhSn(<i>o</i> -Tol) ₃	PhSnCl ₃ / <i>o</i> -Tol)MgBr THF; RT (10) + refl. (10)	EtOH/toluene	94	166–167	C ₂₇ H ₂₆ Sn 469.19	68.95 (69.12) 5.62 (5.59)
Ph ₃ Sn(<i>m</i> -Tol)	Ph ₃ SnCl/ <i>m</i> -Tol)MgBr THF; RT (10) + refl. (10)	EtOH/toluene	80	122–123	C ₂₅ H ₂₂ Sn 441.14	67.98 (68.07) 4.98 (5.03)
Ph ₂ Sn(<i>m</i> -Tol) ₂	Ph ₂ SnCl ₂ / <i>m</i> -Tol)MgBr THF; RT (10) + refl. (10)	EtOH	85	91–92	C ₂₆ H ₂₄ Sn 455.17	68.52 (68.61) 5.57 (5.31)
PhSn(<i>m</i> -Tol) ₃	PhSnCl ₃ / <i>m</i> -Tol)MgBr THF; RT (10) + refl. (10)	EtOH/toluene	63	106	C ₂₇ H ₂₆ Sn 469.19	68.84 (69.12) 5.43 (5.59)
Ph ₃ Pb(<i>o</i> -Tol)	Ph ₃ PbI/ <i>o</i> -Tol)MgBr ether; RT (4) + refl. (12)	EtOH/toluene	57	171–175	C ₂₅ H ₂₂ Pb 529.65	55.67 (56.69) 4.19 (4.19)
Ph ₂ Pb(<i>o</i> -Tol) ₂	Ph ₂ PbI ₂ / <i>o</i> -Tol)MgBr ether; RT (2) + refl. (14)	EtOH	27	136–137	C ₂₆ H ₂₄ Pb 543.68	57.29 (57.44) 4.37 (4.45)
PhPb(<i>o</i> -Tol) ₃	(<i>o</i> -Tol) ₃ PbBr/PhMgBr ether; RT (3) + refl. (14)	EtOH/toluene	65	151–153	C ₂₇ H ₂₆ Pb 557.70	58.20 (58.15) 4.69 (4.70)
Ph ₃ Pb(<i>m</i> -Tol)	Ph ₃ PbCl/ <i>m</i> -Tol)MgBr THF; RT (48) + refl. (10)	EtOH/toluene	27	145	C ₂₅ H ₂₂ Pb 529.65	56.20 (56.69) 4.38 (4.19)
Ph ₂ Pb(<i>m</i> -Tol) ₂	Ph ₂ PbI ₂ / <i>m</i> -Tol)MgBr THF; RT (2) + refl. (12)	EtOH	90	95	C ₂₆ H ₂₄ Pb 543.68	57.30 (57.44) 4.35 (4.45)
PhPb(<i>m</i> -Tol) ₃	(<i>m</i> -Tol) ₃ PbCl/PhMgBr THF; RT (72) + refl. (10)	EtOH	31	106	C ₂₇ H ₂₆ Pb 557.70	58.00 (58.15) 4.64 (4.70)

^a Abbreviations: RT is the ambient temperature, refl. the refluxing solvent.^b Ref. [22].^c Chromatographic purification on silica gel.^d 150°C.^e Chromatographic separation on silica gel, four fractions (1:5:6:12). Fraction 1 (m.p. 160–170°C), 2 (m.p. 218–224°C, pure Si(*o*-Tol)₄), 3 (colorless oil), 4 (colorless oil of high viscosity). Ref. [23] describes five stereoisomers: m.p. 145 (detail), 228 (detail), 270, 300 and 344°C. Ref. [24]: m.p. 228–230°C.^f Compound contaminated with Ge₂(*p*-Tol)₆.

Table 5. Summary of crystal data, intensity data collection (Mo radiation, ambient temperature) and refinement for Ph₃Sn(*o*-Tol) and PhSn(*o*-Tol)₃

	Ph ₃ Sn(<i>o</i> -Tol)	PhSn(<i>o</i> -Tol) ₃
Cryst. syst., space group	tetragonal, P4 ₂ c	tetragonal, P4 ₂ c
Unit cell dimen.: <i>a</i> , <i>c</i> (Å) ^a	12.002(3), 7.204(4)	12.032(1), 7.853(2)
<i>V</i> (Å ³), <i>Z</i> , <i>F</i> (000)	1038(2), 2, 444	1136(1), 2, 476
<i>D</i> _{calcd.} , <i>D</i> _{exptl.} (g cm ⁻³)	1.411, 1.407	1.372, 1.372
sin θ_{\max} /0.71069 (Å ⁻¹)	0.595	0.704
Refl.: meas., indep. (int. <i>R</i>)	3696, 767(0.102)	3664, 1340(0.026)
Refl.: used, limit	273, <i>I</i> > 1 σ (<i>I</i>)	682, <i>I</i> > 1 σ (<i>I</i>)
Variab., ratio refl./var.	36, 7.6	35, 19.5
Final <i>R</i>	0.0915	0.0542

^a Ph₄Sn: *a* = 12.058(1), *c* = 6.581(1) Å, *V* = 957 Å³; Sn(*o*-Tol)₄: *a* = 12.021(1), *c* = 8.054(1) Å, *V* = 1164 Å³ (see Ref. [17]).

Acknowledgements—We gratefully acknowledge financial support from the Deutsche Forschungsgemeinschaft, Bonn, Germany and the Fonds der Chemischen Industrie, Frankfurt/Main, Germany. C. D. thanks the European Community for a grant under the Erasmus scheme.

REFERENCES

- Part 4: Charissé, M., Mathiasch, B., Dräger, M. and Russo, U., *Polyhedron*, 1995, **14**, 2429.
- Charissé, M., Roller, S. and Dräger, M., *J. Organomet. Chem.*, 1992, **427**, 23.
- Charissé, M., Gauthey, V. and Dräger, M., *J. Organomet. Chem.*, 1993, **448**, 47.
- Schneider-Koglin, C., Mathiasch, B. and Dräger, M., *J. Organomet. Chem.*, 1994, **469**, 25.
- Chieh, P. C., The fact that the molecules become flatter as the central atom becomes larger has been mentioned first for the homoleptic series Ph₄M (M = C, Si, Ge, Sn), *J. Chem. Soc. Dalton Trans.*, 1972, 1207.
- Hunter, C. A. and Sanders, K. M., A π - π interaction model for porphyrins, *J. Am. Chem. Soc.*, 1990, **112**, 5525.
- Dance, I. G. and Scudder, M. L., An attractive nonbonded phenyl-phenyl association scheme in a series of [Ph₄P]⁺ crystal structures, *Chem. Eur. J.*, 1996, **2**, 481.
- Harris, R. K., Kennedy, J. D. and McFarlane, W., Sagging pattern ("U" shaped appearance) in heteronuclear chemical shifts in series of heteroleptic compounds, In *NMR and the Periodic Table*, ed. R. K. Harris and B. E. Mann. Academic Press, London, 1978, p. 314.
- Harris, R. K., Kennedy, J. D. and McFarlane, W., In *NMR and the Periodic Table*, ed. R. K. Harris and B. E. Mann. Academic Press, London, 1978, p. 346.
- Harris, R. K., In *The Multinuclear Approach to NMR Spectroscopy*, ed. J. B. Lambert and F. G. Riddell. Reidel Publ. Comp., Dordrecht, 1982, p. 354.
- Harris, R. K., Kennedy, J. D. and McFarlane, W., First tabulation of ⁷³Ge NMR data, In *NMR and the Periodic Table*, ed. R. K. Harris and B. E. Mann. Academic Press, London, 1978, p. 340.
- Kennedy, J. D. and McFarlane, W., tabulation of ⁷³Ge NMR data, In *Multinuclear NMR*, p. 310, Ed. Mason, J., Plenum Press, New York, 1987.
- Kennedy, J. D. and McFarlane, W., In *Multinuclear NMR*, ed. J. Mason, Plenum Press, New York, 1987, p. 310.
- Schmidbaur, H. and Rott, J., *Z. Naturforsch. B*, 1990, **45**, 961.
- Liepins, E., Petrova, M. V., Bogorodovskii, E. T. and Zavgorodnii, V. S., *J. Organomet. Chem.*, 1991, **410**, 287.
- Takeuchi, Y., Popelis, J., Manuel, G. and Boukherroub, R., recent ⁷³Ge NMR data, *Main Group. Met. Chem.*, 1995, **18**, 191.
- Belsky, V. K., Simonenko, A. A., Reikhsfeld, V. O. and Saratov, I. E., *J. Organomet. Chem.*, 1983, **244**, 125.
- Stewart, J. J. P., *J. Comput. Chem.*, 1989, **10**, 221.
- Stewart, J. J. P., *J. Comput. Chem.*, 1991, **12**, 320.
- Mealli, C. and Proserpio, D. M., Program CACAO (Computer Aided Composition of Atomic Orbitals), *J. Chem. Educ.*, 1990, **67**, 399.
- π -HOMO \rightarrow π^* -LUMO transitions are the familiar UV bands of the tetraaryls: Gouterman, M. and Sayer, P., *J. Mol. Spectrosc.*, 1974, **53**, 319.
- Gilman, H. and Smart, G. N. R., *J. Org. Chem.*, 1950, **15**, 720.
- Smart, G. N. R., Gilman, H. and Otto, H. W., 5 different isomers of Si(*o*-Tol)₄, data for 2 isomers in detail, *J. Am. Chem. Soc.*, 1955, **77**, 5193.
- Hutchings, M. G., Maryanoff, C. A. and Mislow, K., ¹H-DNMR of Si(*o*-Tol)₄, *J. Am. Chem. Soc.*, 1973, **95**, 7158.
- Hutchings, M. G., Andose, J. D. and Mislow, K., Force field calculations of tetraarylmethanes and silanes, *J. Am. Chem. Soc.*, 1975, **97**, 4553.
- Rocha, J. and Klinowski, J., *Angew. Chem.*, 1990, **102**, 539.
- Rocha, J. and Klinowski, J., *Angew. Chem. Int. Ed. Engl.*, 1990, **29**, 553.

28. Harris, R. K. and Sebal, A., *Mag. Reson. Chem.*, 1987, **25**, 1058.
29. Sebal, A. and Harris, R. K., *Organometallics*, 1990, **9**, 2096.
30. Ascenso, J. R., Harris, R. K. and Granger, P., $\delta(^{207}\text{Pb}) = -135$ ppm for solid $\text{Pb}(\text{p-Tol})_4$, *J. Organomet. Chem. C*, 1986, **301**, 23.